

## Alloy Formation in Pt–Sn–Alumina Catalysts: *In Situ* X-Ray Diffraction Study

RAM SRINIVASAN,<sup>†</sup> ROBERT J. DE ANGELIS,<sup>\*</sup> AND BURTRON H. DAVIS<sup>\*,†</sup>

<sup>\*</sup>Department of Metallurgical Engineering and Materials Science, University of Kentucky, Lexington, Kentucky 40506; and <sup>†</sup>Kentucky Energy Cabinet Laboratory, P.O. Box 13015, Lexington, Kentucky 40512

Received August 5, 1986; revised March 10, 1987

Changes in Pt–Sn–alumina catalysts, prepared from the  $(\text{Pt}_3\text{Sn}_8\text{Cl}_{20})^2$  complex, during reduction in flowing hydrogen were followed by *in situ* X-ray diffraction (XRD). For high metal loading (ca. 5% Pt) evidence was found for both Pt–Sn and Pt phases; other Pt–Sn phases, such as  $\text{Pt}_3\text{Sn}$ ,  $\text{PtSn}_2$ , and  $\text{PtSn}_4$ , were not observed. Metallic Pt was detected for a 0.6 wt% Pt– $\text{Al}_2\text{O}_3$  catalyst but only a Pt–Sn alloy was observed for a 0.6 wt% Pt catalyst containing Sn. *In situ* XRD studies therefore support alloy formation with a stoichiometry of Pt:Sn = 1:1; the Sn in excess of that needed to form this alloy is present in an X-ray “amorphous” form. © 1987 Academic Press, Inc.

### INTRODUCTION

Bimetallic catalysts have been of interest in heterogeneous catalysis for a long time. Schwab, in a classic paper (1), called attention to the role of alloy composition in determining catalytic activity. The electronic theory of catalysis (2, 3) provided motivation for numerous studies with alloy catalysts during the 1950s. Introduction of the Pt–Re naphtha reforming catalysts by Chevron in the 1960s (4) provided additional motivation for the study of supported bimetallic catalysts.

Many early investigators held the view that *d*-band electron concentration could be controlled by alloy formation so that catalytic selectivity and/or activity could be influenced through control of the *d*-band electron concentration (5). Much of the early work utilized unsupported metal alloys (6). Many workers used concepts based upon alloy formation to explain the results from their studies of supported bimetallic catalysts (e.g., Refs. (7, 8)). As more studies were completed with supported bimetallic catalysts, workers began to question the extent of alloy formation in these catalysts. This was especially true in

those cases where, under normal circumstances, the two metals were immiscible over some, or all, of the compositional range. Thus, Sinfelt (9) introduced the concept of metal clusters, without specifying a cluster composition, to account for the properties of supported bi- or polymetallic catalysts.

Two frequently studied catalysts have Pt–Sn or Pt–Re as the bimetallic components. In both systems, evidence has been provided to support either alloy formation (10–12) or the absence of alloys (13, 14). In the cases of both Pt–Re and Pt–Sn there are reports that Re or Sn is not reduced to the metallic state; more specifically, two groups, Adkins and Davis (15) and Sexton *et al.* (16), reported X-ray photoelectron spectroscopy (XPS) data that showed the tin atoms observable by this technique were not present in the metallic state even if the Group VIII noble metal was in the metallic state. XPS studies also indicated that Re was not in the metallic state in Pt–Re catalysts (14, 17). These XPS data were in conflict with extensive experimental data that were believed to be consistent with alloy formation.

Aromatic selectivity data from alkene

dehydrocyclization using Pt–Sn catalysts provides indirect evidence for alloy formation (8). Additional indirect evidence for the state of Pt and Sn has been obtained from temperature-programmed reduction results (18).

Lieske and Volter (19) concluded, based upon temperature-programmed reduction and adsorption of oxygen or hydrogen, that (1) a minor part of the tin is reduced to the metal and this forms “alloy” clusters, (2) the major part of the tin is only reduced to the Sn(II) state, (3) the reduction of Sn(IV) is catalyzed by Pt, and (4) the amount of alloyed tin increases with increasing tin or platinum content.

Direct evidence for Pt–Sn alloy formation has been obtained from Mössbauer studies (20–23); however, many of these studies were at high metal loadings and even then such a complex spectrum was obtained that there was some uncertainty in assigning Sn metal to the exclusion of some tin oxide phase. However, Mössbauer results clearly show changes upon reduction which demonstrate the reduction of Sn(IV) but the width of the peaks for the reduced sample prevents, in general, a specific assignment of compounds. This is exemplified by the results of Kuznetsov *et al.* (24) who reported that Pt–Sn– $\gamma$ -Al<sub>2</sub>O<sub>3</sub> catalysts are multicomponent; that is, they have highly dispersed products of the chemical interactions of Sn(IV), Sn(II), and Sn(0) with both support surface and Pt. Pt, according to these authors, forms nearly all possible alloys with Sn. These results support earlier Mössbauer data, and the models of Pt–Sn–Al<sub>2</sub>O<sub>3</sub> catalyst based upon them (25).

Davis (26) prepared supported Pt–Sn catalysts using an acetone solution of a bimetallic complex of [Pt<sub>3</sub>Sn<sub>8</sub>Cl<sub>20</sub>]<sup>2–</sup> and subsequently used these catalysts for alkane dehydrocyclization studies. These catalysts usually retained 90% or more of the chlorine added during the impregnation following reduction at 550°C in flowing hydrogen and use as a dehydrocyclization

catalyst at 482°C. Yermakov and Kuznetsov (27) summarized work, primarily from their laboratory or from research groups collaborating with them, on the preparation of supported metallic catalysts by the decomposition of organometallic complexes; among the preparations for supported Pt–Sn catalysts was included the use of acetone solutions of H<sub>4</sub>[Pt<sub>3</sub>Sn<sub>8</sub>Cl<sub>20</sub>]. Among the conclusions of these authors were the following: (1) data from Mössbauer spectroscopy showed that metallic tin was not formed after reduction of the Pt–Sn surface complex and (2) two types of Sn(II) ions were observed. One type appeared to be bound to the support and the other type was bound to both the support and the Pt atoms. These authors also reported some amazing catalytic properties: catalysts prepared via [Pt(SnCl<sub>3</sub>)Cl<sub>2</sub>]<sup>2–</sup> produced 60% benzene with respect to hexane converted while a catalyst prepared using [Pt(SnCl<sub>3</sub>)<sub>5</sub>]<sup>3–</sup> yielded, at 500°C, 80% hexene with respect to hexane converted! The latter authors and co-workers (24, 28, 29) provided additional characterization data to support their model for the chemical state of the supported metals.

In a related bimetallic catalytic system, Ni–Sn–SiO<sub>2</sub>, Swift and Bozik (30) reported that X-ray diffraction (XRD) revealed the presence of nickel and nickel–tin alloy phases. Swift and co-workers (31) showed that tin oxide supported on silica could be reduced by hydrogen to the metal and could then be reoxidized to SnO<sub>2</sub>.

Bouwman *et al.* (32) obtained Auger spectroscopic results which showed that the surface of unsupported Pt–Sn and Pt<sub>3</sub>Sn alloys became enriched in tin when they were annealed under vacuum. Adsorption of oxygen on the alloys caused a further enrichment in tin above the annealed state and severe oxidation led to complete disappearance of Pt from the surface. Reduction at 500°C in hydrogen resulted in surface enrichment in Pt above that of the annealed surface concentration. Hoflund *et al.* (33) obtained ISS results which sug-

gested that oxygen interacts with the Pt and not the tin in a  $\text{Pt}_3\text{Sn}$  alloy; however, these authors do caution that this is a complex system. The ESCA results of Adkins and Davis (15) point to just the opposite view. Sn, at least the fraction present in the surface layer sensitive to ESCA measurements, is in an oxidized state even though the Group VIII metal was in the zero valence state.

Richter and Bornmann (34) demonstrated, using *in situ* XRD, that the Pt (311) peak was appropriate for characterization by X-ray diffraction technique but that the assumption of the absence of lattice distortions was not valid. Ushakov and Moroz (35) utilized *in situ* XRD and concluded that only half of the Pt on an alumina support was reduced in hydrogen at 500°C; the other half was ionic Pt bonded to the support or a highly dispersed state of zero-valent Pt. In this study, we have utilized an *in situ* X-ray diffraction technique in yet another attempt to better define this important catalyst system.

#### EXPERIMENTAL

**Catalysts.** The support material used in this investigation is nonporous Degussa alumina oxide C with a surface area of 110  $\text{m}^2/\text{g}$ . A 0.6 wt% Pt catalyst was prepared by an incipient wetness technique, using an aqueous solution of  $\text{PtCl}_2$ . Supported Pt-Sn catalysts were prepared by impregnating the support, which had been previously calcined in air at 550°C, with an acetone solution of a Pt-Sn complex,  $[(\text{C}_2\text{H}_5)_4\text{N}]_2\text{Pt}_3\text{Sn}_8\text{Cl}_{20}$ , prepared according to a published procedure (36). The excess acetone solvent was removed by evaporation in air prior to drying at 120°C. This preparation procedure was the one utilized in our earlier studies (8, 15, 26).

**XRD.** The catalyst sample was pressed into a stainless-steel holder as a 1-mm-thick, 19-mm-diameter disk. The sample was mounted into a diffraction camera with the capability of *in situ* high-temperature (to ca. 800°C) operation at one atmosphere

of hydrogen pressure. The camera was mounted on a Picker X-ray diffractometer. This technique ensures that the X-ray beam samples the same portion of each catalyst for all treatments. The X-ray source was a nickel target X-ray tube, operated at 35 kV and 8 mA. Reductions were carried out by heating the sample to the desired temperature at a rate of ca. 2°C/min in hydrogen flowing at ca. 0.05 liter/min. After a reduction period the sample was cooled to room temperature in a 0.02 liter/min flow of helium. The X-ray data were collected using 1/15, 1/30, or 1/60 degree steps with a counting time of 50 or 100 s/step, depending upon the  $2\theta$  range of interest.

#### RESULTS

The two most intense metallic Pt(111) and (200) peaks have  $2\theta$  values that partially overlap with more intense alumina peaks; this makes it impossible to observe these peaks in the present experimental study. However, the Pt(311) peak is observable since it is not influenced by the overlap of any alumina peaks. This profile has therefore been utilized to identify the presence of metallic Pt in the Pt- $\text{Al}_2\text{O}_3$  catalyst (Figs. 1 and 2). After reduction at either 400 or 500°C, a broad Pt(311) peak is observed in the XRD patterns. The crystal-

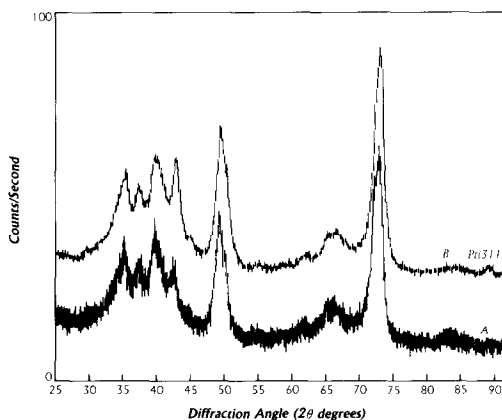


FIG. 1. X-ray diffraction patterns for 0.6% Pt on Degussa alumina: (A) after calcination at 500°C for 4 h; and (B) after reduction at 500°C for 7 h.

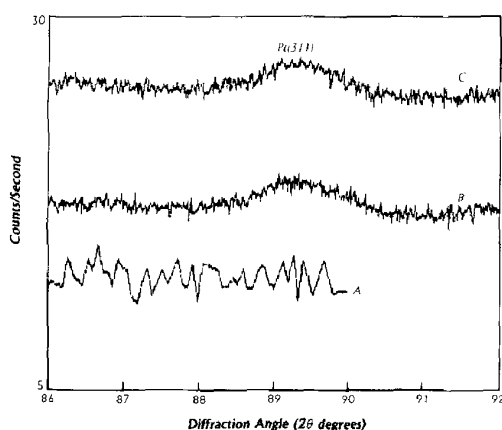


FIG. 2. X-ray diffraction patterns ( $2\theta = 86$  to  $92^\circ$ ) for (A) Degussa alumina after calcination at  $500^\circ\text{C}$ , (B) 0.6 wt% Pt on Degussa alumina after reduction at  $400^\circ\text{C}$  for 7 h, and (C) sample from B after reduction for 7 h at  $500^\circ\text{C}$ .

lite size calculated from the line width at half-maximum intensity is in the range of 90–100 Å for a material reduced at  $500^\circ\text{C}$ .

Attempts made to record a XRD pattern for the  $(\text{Pt}_3\text{Sn}_8\text{Cl}_{20})^{-2}$  cluster present in the tetraethylammonium salt did not produce a X-ray diffraction pattern. Lindsay *et al.* (37) was also unable to obtain a diffraction pattern for this complex; apparently the

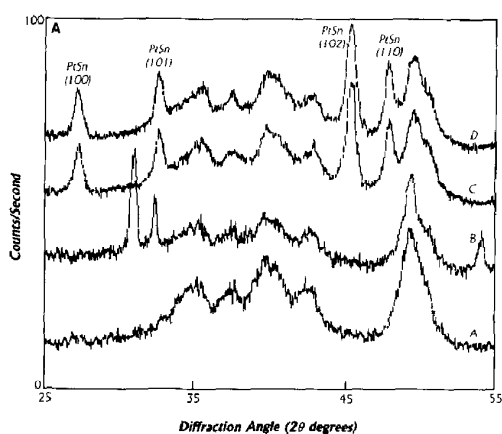


FIG. 3A. X-ray diffraction patterns ( $2\theta = 25$  to  $55^\circ$   $\text{NiK}\alpha$  radiation) for (A) Degussa alumina catalyst support after calcination for 4 hr at  $500^\circ\text{C}$ , (B) 5% Pt prepared from  $(\text{Pt}_3\text{Sn}_8\text{Cl}_{20})^{-2}$  complex after drying at  $120^\circ\text{C}$ , (C) sample from B after 8 h of reduction at  $400^\circ\text{C}$ , and (D) sample C after 6 h of reduction at  $550^\circ\text{C}$ .

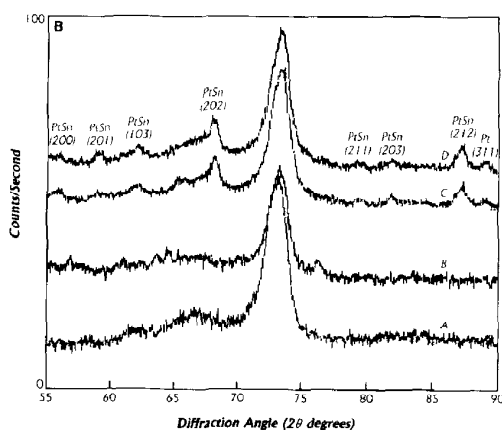


FIG. 3B. X-ray diffraction patterns ( $2\theta = 55$  to  $90^\circ$ ) for samples shown in Fig. 3A. (See Fig. 3A for sample identifications.)

unsupported salt complex is an amorphous solid.

The catalyst containing a nominal 5 wt% Pt, initially as a  $(\text{Pt}_3\text{Sn}_8\text{Cl}_{20})^{-2}$  complex on  $\text{Al}_2\text{O}_3$ , has a XRD pattern that contains three prominent peaks in addition to those from the alumina support (Figs. 3A and 3B, curve B). The XRD patterns (Figs. 3A and 3B, curves C and D) obtained for this material after reduction at 400 and  $500^\circ\text{C}$  were very different from the pattern of the starting material. There are eight peaks in the XRD patterns from the reduced material that closely agree with the  $2\theta$  positions reported for an alloy with equal molar composition of platinum and tin (Pt–Sn) (Table 1). The relative intensities and  $2\theta$  positions for diffraction peaks for catalysts prepared from the platinum–tin complex are shown in Fig. 4 (peaks, represented by dashed line, were present but intensity could not be accurately measured because of interference by alumina peaks). It appears that during the reduction process a Pt–Sn intermetallic is formed even though the original complex had a molar ratio of Pt:Sn that was nearly 1:3. The tin in excess of that required to form Pt–Sn was not observed either as tin oxide or as metallic tin. If tin is present in either of these forms, the crystallite size must be less than about 2.0 nm,

TABLE I

Peak Positions and Relative Intensities for Various Pt-Sn Alloys and the Supported Pt-Sn-Al<sub>2</sub>O<sub>3</sub> Catalysts

Phase	2	<i>I</i> (%)	2	<i>I</i> (%)	2	<i>I</i> (%)	2	<i>I</i> (%)	2	<i>I</i> (%)
Pt <sub>3</sub> Sn	42.02	100	48.91	53	71.67	30	86.7	30	—	—
Pt-Sn	27.3	60	32.62	70	45.29	100	47.59	80	87.25	90
Pt-Sn <sub>2</sub>	25.78	50	42.89	70	62.50	80	78.63	100	—	80
Pt-Sn <sub>4</sub>	16.72	85	33.03	100	34.74	100	37.68	100	45.87	100
5% Pt-Sn/ Al <sub>2</sub> O <sub>3</sub>	27.25	59	32.62	69.3	45.29	100	47.59	76	87.20	33
0.6% Pt-Sn/ Al <sub>2</sub> O <sub>3</sub>	27.29	61	32.60	77	45.28	100	—	—	87.25	36

below the XRD detection limit. Thus, at least approximately 65% of the tin present in the reduced catalyst is in a form that is not detected by XRD.

XRD scans in the region of the Pt(311) peak are shown in Fig. 5. Although the curves A and B in Fig. 5 do not cover the full  $2\theta$  range of curve C, it is evident that Pt is present in the 5 wt% Pt catalyst in both Pt-Sn and Pt forms. The Pt-Sn peak corresponds to approximately 70% of the Pt-Sn plus Pt(311) peaks for reductions at both 400 and 550°C. The Pt crystallite size, calculated from the half-width of the

Pt(311) peak in Fig. 5, is approximately 15 nm. A similar calculation made for the Pt-Sn(212) peak gave a particle size of 13.5 nm. It is apparent from the data in Table 2 and from the shapes of the Pt-Sn peaks in Fig. 6 that the crystallite sizes calculated from each of the five Pt-Sn peaks are similar; this is a strong indication that the crystallites have isotopic shapes.

A 0.6 wt% Pt catalyst, with Pt added as the (Pt<sub>3</sub>Sn<sub>8</sub>Cl<sub>20</sub>)<sup>-2</sup> complex, was reduced at 400 and then at 500°C in flowing hydrogen. Diffraction patterns of the reduced material (Fig. 7 curve A, and Fig. 8 curves B and C)

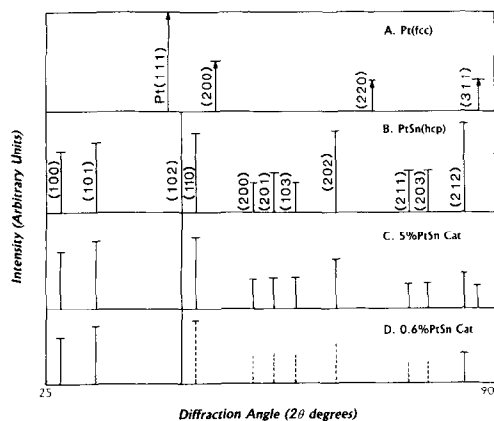


FIG. 4. Diffraction peak positions and relative intensities for (A) Pt (fcc), (B) Pt-Sn (hcp), (C) a reduced Pt-Sn-alumina catalyst with 5 wt% Pt, and (D) reduced Pt-Sn-alumina catalyst with 0.6 wt% Pt.

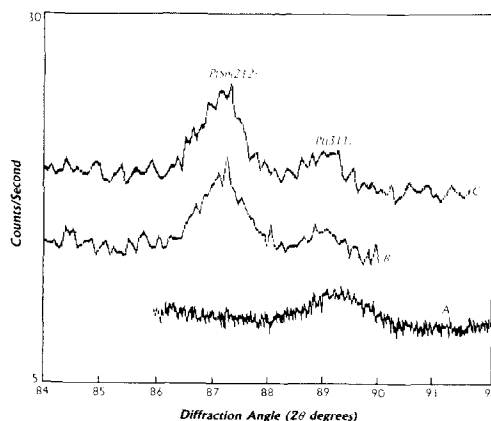


FIG. 5. X-ray diffraction patterns for (A) 0.6 wt% Pt only on alumina after 7 h of reduction at 500°C, (B) 5 wt% Pt in Pt-Sn-alumina catalyst after reduction at 400°C for 8 h, and (C) B after reduction at 550°C for 6 h.

TABLE 2  
Crystallite Size for 5 wt% Pt as Pt-Sn Alloy in the Catalysts Reduced at 400 or 550°C

Catalyst	Crystallite size (Å) at 2θ for				
	27.3	32.6	45.3	47.6	87.3
400°C reduction	150	112	146	147	138
550°C reduction	140	140	145	150	133

provide evidence that reduction caused alloy formation. The diffraction pattern from the reduced material indicates that Pt-Sn alloy is formed even at this lower metal loading. The Pt-Sn peak observed at  $2\theta = 87.4$  is very broad and there is no indication in the pattern of the Pt(311) peak at  $2\theta = 89.1$ . The Pt-Sn intermetallic crystallite size of 45 Å was estimated from the Pt-Sn(212) diffraction line. In making these calculations, peak regions such as  $2\theta = 84$  to 92 were recorded on an expanded  $2\theta$  scale to permit a more accurate measurement of the line width. It is also apparent from the pattern in Fig. 7, curve B, that reoxidation at 500°C for 10 h eliminated the Pt-Sn alloy peaks; however, peaks that could be attributed to an oxide of platinum

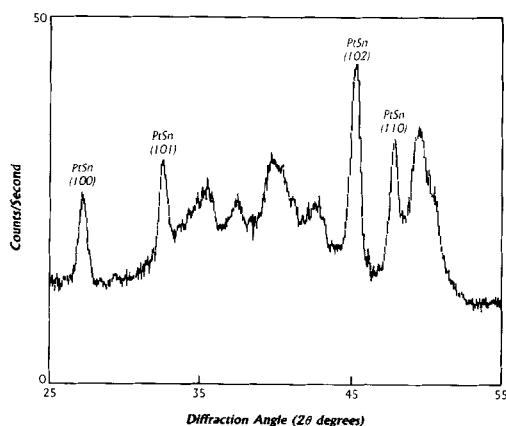


FIG. 6. X-ray diffraction pattern ( $2\theta = 25$  to  $55^\circ$ ) for the 5 wt% Pt in Pt-Sn-alumina after reduction at 550°C for 6 h.

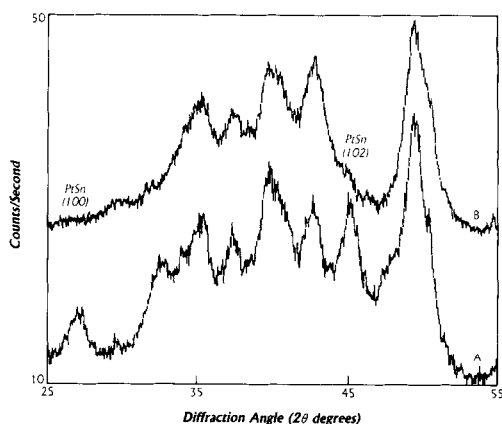


FIG. 7. X-ray diffraction patterns for the 0.6 wt% Pt in Pt-Sn-alumina catalysts: (A) reduced at 500°C for 6 h and (B) pattern of sample A after reoxidation at 500°C for 10 h.

or tin or of a mixed metal oxide phase were not observed in the reoxidized sample.

## DISCUSSION

The XRD data make it clear that Pt-Sn alloy is present in a reduced catalyst. The platinum-tin alloy, or at least the predominant and the only alloy detected, has a composition of Pt-Sn. Comparing the areas

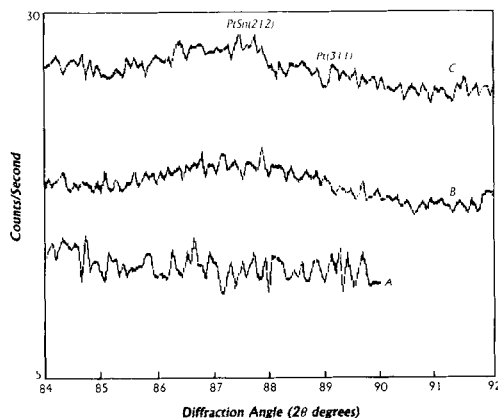


FIG. 8. X-ray diffraction patterns ( $2\theta = 84$  to  $92^\circ$ ) for (A) Degussa alumina after calcination at 500°C for 4 h, (B) 0.6 wt% Pt in Pt-Sn-alumina after reduction at 400°C for 5 h, and (C) sample from B after reduction at 500°C for 6 h.

of the Pt(311) and the Pt-Sn peak at  $2\theta = 87.4^\circ$ , one can make a rough estimate that XRD is detecting roughly the same amount of Pt in the 0.6 wt% Pt-Sn catalyst as in the catalyst with 0.6% Pt only. Thus, nearly two of every three tin atoms must be present in a form other than an alloy. However, no other form of Sn was detected by XRD.

The literature presents a long history of the difficulty of detecting Pt metal by XRD when an alumina support is present. As one approach to this problem, the alumina support was dissolved in acetylacetone, the platinum metal residue was collected by filtration, and the crystallite size was then determined by XRD using the Pt(111) peak that was no longer masked by the very large alumina peak (38). In another approach, van Nostrand (39), using separately measured relative intensities for alumina or platinum, constructed a series of theoretical standard curves for a number of metal loadings up to 1 wt% Pt and for various Pt crystal sizes for several Pt loadings. The crystallite size for a supported Pt catalyst was obtained by matching the XRD curve of the supported catalyst to the standard curve with a similar Pt loading. These are just two examples of the difficulty encountered in detecting Pt metal in Pt-alumina catalysts that contain less than about 1 wt% Pt. While this does not provide an absolute proof, it does strongly support the view that if an XRD third-order reflection peak of Pt is observed with a 0.6 wt% Pt-alumina catalyst it must represent all, or at least a large fraction, of the Pt present in the sample. We cannot imagine a scenario that would provide sufficient XRD intensity for the Pt observed in the present study to represent the large-size tail of a wide range of Pt particle sizes. Furthermore, Pt crystallites in the order of 100 Å following reduction at 500°C should not be surprising when it is considered that the support is comprised of nonporous alumina.

Two groups (15, 16) reported XPS data which indicated that Sn was not in a metallic state in reduced Pt-Sn-alumina cat-

alysts. Adkins and Davis (15) used an AEI 200 spectrometer to obtain their published results. This instrument employs an oxygen-containing vacuum pump oil and this could conceivably be a source of oxygen. However, reduction of a portion of the same catalyst preparation used by Adkins and Davis in a Leybold-Heraeus instrument that utilizes cryogenic turbo pumping and titanium getter pumps to maintain high vacuum conditions again indicated that metallic Sn was not present in quantities detectable by XPS. The current results make it clear that Pt-Sn metal alloy should have been present during the XPS studies by Adkins and Davis even though all their efforts to obtain XPS evidence for metallic Sn failed. The XRD results are, however, not inconsistent with a major fraction of the added tin being present as an eggshell of tin aluminate as proposed by Adkins and Davis (15). However, the model proposed in Ref. (15) would have to be altered to show a supported Pt-Sn intermetallic instead of, or in addition to, Pt crystallites.

The XRD data are in conflict with our earlier XPS results. In view of the excellent match between the Pt-Sn alloy pattern, in terms of peak positions and the relative intensities, and the XRD patterns for the supported catalysts, it appears certain that an alloy is formed during the reduction of this catalytic material. In this respect the XRD data agree with the Mössbauer spectroscopic results obtained with higher metal loadings (5% Pt or greater). In light of these direct measures of Pt-Sn intermetallics, we are compelled to accept that an alloy is formed in supported Pt-Sn catalysts. The XRD data indicate that the alloy is Pt-Sn; this is the phase expected from the phase diagram (40).

The problem at present is to reconcile the XPS data with alloy formation. Similar XPS results have been obtained in three laboratories and these provide no evidence for metallic tin. Bouwman and Biloen (41) provide convincing evidence for surface

enrichment by Sn for unsupported Pt–Sn alloys; surface enrichment by Sn is greatest when the material has been exposed to oxygen. Hegde and Sinha (42) summarize data to show surface enrichment by tin for a number of alloys. Thus, XPS should detect more Sn than Pt in the surface of the supported alloy crystals. Tin is readily oxidized and it is easily conceived that the Sn-enriched surface layer could be essentially tin oxide. However, XPS data from the supported rhodium–tin catalysts indicated that Rh was present in the metallic state but the tin was in an oxidized state (15). Furthermore, Pt–Sn on a carbon support was indicative of reduced Pt (15). Even if a tin-enriched surface layer was oxidized, the amount of tin in the bulk alloy should still be nearly as great as that of Pt or Rh. Thus, if metallic Rh is detected by XPS, a like amount of metallic tin should be observed but this was not the case.

A very speculative explanation of the XPS results requires oxidation of the tin-enriched surface layer. Subsequently, bulk migration of Sn to the surface to form additional tin oxide would leave the original Pt–Sn intermetallic crystallites depleted in Sn, and enriched in metallic Pt. The XPS spectrum would then be comprised of only ionic Sn on the support surface plus the oxidized tin present on the original Pt–Sn intermetallic crystallites. The tin oxide layer supported upon the Pt-rich skeleton of the original Pt–Sn crystal would be required to be thin enough for the Rh 3d electrons, and Pt 4f electrons with the carbon-supported catalyst, to escape through the tin oxide surface layers. For the 0.6 wt% Pt catalyst with tin, the intermetallic crystal surface area and the tin concentration appear to permit such a structure to be formed. Since the 5 wt% Pt catalyst contains both Pt and Pt–Sn crystals, such calculations are, at present, meaningless. If this explanation is correct, each of the three XPS instruments at three different locations must have sufficient residual oxygen to permit reoxidation of the

tin in the supported catalysts. However, a level of 1 to 3 ppm oxygen in the helium gas flow in the XRD instrument did not permit reoxidation of a detectable fraction of the Pt–Sn alloy formed during reduction. High temperature (500°C) reoxidation of the Pt–Sn alloy renders the metallic phases amorphous to XRD. This attempt to reconcile the XPS and XRD data for supported Pt–Sn catalysts requires a number of special circumstances. While we consider this unlikely, we are unable to advance, at this time, a more appealing explanation.

It now appears certain that the presence of Pt–Sn alloys in supported catalysts has been confirmed by *in situ* X-ray diffraction even with a loading of Pt as low as 0.6 wt%. At this time, it is not possible to quantitatively define the fraction of Pt observed by the XRD technique. However, the peak area of the 0.6 wt% Pt–Sn alloy at  $2\theta = 87.1$  is approximately equal to the size of the Pt(311) peak of the catalyst containing 0.6 wt% Pt only; this suggests that a large fraction of Pt is present as an alloy. In addition, it can be seen from the intensity of the XRD peaks that a large fraction of the Pt should have been detected.

It appears that low-metal-loaded supported Pt–Sn catalysts have Pt present predominantly as 1 : 1 Pt : Sn alloy. The excess tin present in the catalyst is present in a form that cannot be detected by X-ray. An eggshell of tin aluminate is a possible form for this tin. The surface tin atoms of the alloy seem to be capable of oxidation even though the Pt or Rh noble metal atoms remain in the reduced state. In the reducing atmosphere of naphtha reforming, it appears that the catalytic property of Pt is modified by alloy formation which supported Pt–Sn catalysts.

#### ACKNOWLEDGMENTS

This research was supported in part by the Commonwealth of Kentucky through the Kentucky Energy Cabinet and the Division of Materials Science, U.S. Department of Energy under Contract DE-AS05-82ER12098.

## REFERENCES

1. Schwab, G. M., *Disc. Faraday Soc.* **8**, 166 (1950).
2. Dowden, D. A., *J. Chem. Soc.* p. 242 (1950).
3. Eley, D. D., "Catalysis and the Chemical Bond." Univ. of Notre Dame Press, Notre Dame, 1954.
4. Jacobson, R. L., Kluksdahl, H. E., McCoy, C. S., and Davis R. W., *Proc. Amer. Petroleum Inst. Div. Ref.* **49**, 504 (1969).
5. Beeck, O., *Disc. Faraday Soc.* **8**, 118 (1950).
6. Dowden, D. A., and Reynolds, P., *Disc. Faraday Soc.* **8**, 184 (1950).
7. Reinacker, G., and Bommer, E. A., *Z. Anorg. Chem.* **242**, 302 (1939).
8. Davis, B. H., *J. Catal.* **46**, 348 (1977).
9. Sinfelt, J. H., "Bimetallic Catalysts: Discoveries, Concepts, and Applications." Wiley, New York, 1983.
10. Bolivar, G., Charcosset, M., Ferty, R., Primet, M., and Tournayan, L., *J. Catal.* **37**, 424 (1975).
11. Wagstaff, N., and Prins, R., *J. Catal.* **59**, 434 (1979).
12. McNicol, B. D., *J. Catal.* **46**, 438 (1977).
13. Burch, R., *Platinum Metals Rev.* **22**, 57 (1978).
14. Short, D. R., Khalid, S. M., Katzer, J. R., and Kelley, M. J., *J. Catal.* **72**, 288 (1981).
15. Adkins, S. R., and Davis, B. H., *J. Catal.* **89**, 371 (1984).
16. Sexton, B. A., Hughes, A. E., and Fogar, K., *J. Catal.* **88**, 466 (1984).
17. Adkins, S. R., and Davis, B. H., in "Catalyst Characterization Science" (M. L. Deviney, and J. L. Gland, Eds.), ACS Symp. Series, Vol. 288, p. 57. Amer. Chem. Soc., Washington, DC.
18. Burch, R., *J. Catal.* **71**, 348 (1981).
19. Lieske, H., and Volter, J., *J. Catal.* **90**, 46 (1984).
20. Bacaud, R., Bussiere, P., and Figueras, F., *J. Catal.* **69**, 399 (1981).
21. Kuznetsov, V. I., Yurchenka, E. N., Belyi, A. S., Zatolokina, E. V., Smolikov, M. A., and Duplyakin, V. K., *React. Kinet. Catal. Lett.* **21**, 419 (1982).
22. Zhang, S., Xie, B., Wang, P., and Zhang, J., *Ts' Us Hua Hseuh Pao* **1**(4), 253 (1980).
23. Li, Y.-X., Zhang, Y. F., and Shia, Y.-F., *J. Catal. (China)* **5**, 311 (1985).
24. Kuznetsov, V. I., Belyi, A. S., Yurchenko, E. N., Smolikov, M. D., Protasova, M. T., Zatolokina, E. V., and Duplyakin, V. K., *J. Catal.* **99**, 159 (1986).
25. Zhang, P., Shao, H., Yang, X., and Pang, L., *J. Catal. (China)* **5**, 101 (1984).
26. Davis, B. H., "Bimetallic Catalyst Preparation." U.S. Patent 3,840,475, October 8, 1974.
27. Yermakov, Yu. I., and Kuznetsov, B. N., *J. Mol. Catal.* **9**, 13 (1980).
28. Zaikovskii, V. I., Kovalchuk, V. I., Ryndin, Yu. A., Plyasova, L. M., Kuznetsov, B. N., and Yermakov, Yu. I., *React. Kinet. Catal. Lett.* **14**, 99 (1980).
29. Zhdan, P. A., Kuznetsov, B. N., Shepelin, A. P., Kovalchuk, V. I., and Yermakov, Yu. I., *React. Kinet. Catal. Lett.* **18**, 267 (1981).
30. Swift, H. E., and Bozik, J. E., *J. Catal.* **12**, 5 (1968).
31. Swift, H. E., Bozik, J. E., and Massoth, F. E., *J. Catal.* **15**, 407 (1969).
32. Bouwman, R., Toneman, L. H., and Holscher, A. A., *Surf. Sci.* **35**, 8 (1973).
33. Hoflund, G. B., Asbury, D. A., Kirsezensztejn, R., and Laitinen, H. A., *Surf. Sci.* **161**, L583 (1985).
34. Richter, K., and Bornmann, P., *Crystal Res. Technol.* **16**, 367 (1981).
35. Ushakov, V. A., and Moroz, E. M., *React. Kinet. Catal. Lett.* **27**, 351 (1985).
36. Lindsay, R. V., Jr., Parshall, J. W., and Stolberg, U. G., *Inorg. Chem.* **5**, 109 (1966).
37. Lindsay, R. V., Jr., private communication.
38. Drake, L., personal communication.
39. Van Nostrand, R. A., Lincoln, A. J., Carnevald, A., *Anal. Chem.* **36**, 819 (1964).
40. Hansen, M., "Constitution of Binary Alloys," p. 1142. McGraw-Hill, New York, 1958.
41. Bouwman, R., and Biloen, P., *Surf. Sci.* **41**, 348 (1974).
42. Hegde, R. I., and Sinha, A. P. B., *Appl. Spectrosc. Rev.* **191** (1983).